SCIENCE CHINA
Information Sciences

• RESEARCH PAPER •

October 2015, Vol. 58 102307:1–102307:15
doi: 10.1007/s11432-015-5324-8

An adaptive path selection model for WSN multipath routing inspired by metabolism behaviors

GONG WeiBing, YANG XiaoLong*, ZHANG Min & LONG KePing

School of Computer & Communication Engineering, University of Science and Technology Beijing, Beijing 100083*, China*

Received December 29, 2014; accepted February 9, 2015; published online July 28, 2015

Abstract In multipath routing of wireless sensor network (WSN), greedy path selection is always prone to cause path oscillation (frequent path changes) between each couple of sensor and sink nodes. To alleviate the side effect, we propose an adaptive path selection model (called a WSN path selection model based on the adaptive response by attractor selection (ARAS) model (WARAS)) inspired by metabolism behaviors of *Escherichia Coli*. The model consists of two main features. The first one is a new formula for a parameter called *path-activity* used to indicate adaptation goodness of multipath traffic transmission in dynamic network environments, which is inversely proportional to absolute value of difference between current path quality and best path quality. The second one is a novel attractor expression for attractors of multi-attractor equations to concretely specify stochastic effect of noise items in the equations on the path selection. Then, in an experimental WSN scenario composed of many source nodes and their shared neighbor nodes, we validate a dynamic-adaptive selection characteristic of the WARAS on distributing loads of the neighbor nodes. Subsequently, we design a path quality probe scheme in a multipath ad hoc on-demand distance vector routing (AODV) protocol. Compared with the greedy path selection through the path quality probe scheme, simulation results show the WARAS can perform better on reducing network delay and the path oscillation.

Keywords WSN, multipath, path selection, metabolism behaviors of Escherichia Coli, AODV

Citation Gong W B, Yang X L, Zhang M, et al. An adaptive path selection model for WSN multipath routing inspired by metabolism behaviors. Sci China Inf Sci, 2015, 58: 102307(15), doi: 10.1007/s11432-015-5324-8

1 Introduction

The wireless sensor network (WSN) multipath routing has been extensively studied because of its advantages on transmission efficiency [1], security [2,3], and network lifetime elongation [4]. Normally, the greedy selection is one of the most straightforward schemes for the multipath routing, which can select the optimal path for the data transmission of each couple of the sensor and sink nodes according to the path metrics, for example, path delay, path length [5], path energy consumption [3,6], and selfishness. However, the greedy selection usually causes the transmission path change frequently. Consequently, the path oscillation not only wastes the processing time of the data source to reorder the disorder arrival packets or update the routing table, but also often leads to the unpredictable network congestion. Thus, to decrease the path oscillation and improve the performance of the greedy path selection in the WSN, a

* Corresponding author (email: yangxl@ustb.edu.cn)

biological model adaptive response by attractor selection (ARAS) [7] is introduced to optimize the greedy path selection.

The path selection process in the WSN multipath routing is analogous to the adaptation process of the *Escherichia Coli* (*E. coli*) [8]. Then, the analogousness can inspire us to optimize the greedy path selection with the ARAS model. Concretely, the transmission quality of each path is analogous to the concentration of one kind of mRNA, and each attractor of the bi-attractor equations is analogous to a stable adaptation state of multipath transmission between each couple of the sensor and sink nodes. Here, the path transmission quality can be expressed by the path metric, for example, the path transmission rate, the path delay, the reliability, or the congestion level. Similarly, a parameter called *activity* in the bi-attractor equations can indicate the adaptation goodness of the multipath transmission between the sensor and the sink nodes to the dynamic network environments, and the noise represents some factors taking the stochastic effect on the path transmission quality. Here, the factors may be the random failure of the network equipment, the short-time burst traffic, the channel noise from the physical layer, and so on. Consequently, the characteristic of the ARAS model for keeping the adaptive state is expected to be able to reduce the path oscillation of the greedy selection, and the stochastic characteristic caused by the noise is expected to be able to help each couple of the sensor and sink nodes to find the adaptive transmission paths.

Inspired by the *E. coli*'s metabolism behaviors, the paper proposes a path selection model, namely a WSN path selection model based on the ARAS model (WARAS), which can make the data transmission adapt to the dynamic network environments. In the proposed model, to express the real-time adaptation goodness of the multipath traffic transmission, we redefine the *activity* as *path-activity*, which takes a new formula inversely proportional to the absolute value of the difference between current path quality and best path quality. Through the analogy between the path transmission quality and the mRNA concentration, we redesign the attractor equations with multidimension extension to achieve the adaptive path selection of WSN multipath routing in the dynamic network environments. Furthermore, to concretely specify the stochastic effect of the noise on the path selection, we derive a novel expression for the attractors of the multi-attractor equations. By supposing the uniform noise in multiple paths between each couple of the sensor and sink nodes, the attractors containing the noise are first deduced. Subsequently, we set up an experimental WSN scenario to validate the dynamic-adaptive characteristic of the proposed model. The scenario is composed of many source nodes and neighbor nodes, and each source node can select its next hop from all the neighbor nodes. Then, a path quality probe scheme is designed and integrated into an AODV multipath routing protocol. Finally, based on the multipath routing, we compare the performance of the WARAS and the greedy path selection about reducing the average network delay and the path oscillation.

2 Related work

In recent years, there have been few studies about the path oscillation of the multipath routing, but we still investigate some past related work. In IEEE 802.11 networks, the frequent changes in the link conditions can cause the variations of the route quality, and then lead to the path oscillation [9]. Still in IEEE 802.11 networks, Ref. [10] validated the route oscillation could also be caused by the reception of many route request packets in a very short time. Besides, the route oscillation problem [11,12] also exists in Border Gateway Protocol (BGP), which is generally triggered by local route policy conflictions. Ref. [11] presented a novel approach to fast check the route oscillation of BGP, and the approach could greatly protect the privacy of each autonomous system (AS) by only sharing of AS network ID. Then, in [12], a BGP-Extended multipath framework was proposed to provide path diversity and backward compatibility. In the framework, the stable policy guidelines based on anti-reflexive policy relations are provided to prevent the route oscillation.

However, in these studies about the path oscillation, the literatures with regard to optimizing the greedy path selection are fewer. Ref. [7] proposed a multipath routing scheme for the overlay networks based on the ARAS model. In the scheme, the mRNA concentration is analogous to the path transmission rate,

and the multi-attractor equations are proposed to model the change in the multipath transmission rates. Then, the *activity* is used to express the adaptation goodness of data transmission in the source nodes. Besides, the scheme classifies the paths between each source and destination pair into one primary path and the other secondary paths [13], and the transmission rate of the primary one is higher than all the secondary ones. Furthermore, to make the selection of the primary path adapt to the changing network environments according to the *activity*, the scheme defines three path selection conditions expressed by three fixed points (1, 0.85, and 0) of the *activity*. The first one is that all the paths should be equally treated, the second one is that the primary path is excellent enough, and the last one is that no suitable path can be selected. According to the first and last conditions, the source can select its primary path in uniform random. According to the second condition, the source continues to keep the primary path. Then, Ref. [7] analyzes the variation relationships between the *activity* and the path transmission rate. Still in the multipath routing of the overlay networks, Ref. [14] proposed that the primary path of a data source should be selected with a probability proportional to the goodness of path transmission (e.g., the path reliability, the congestion level, the path security). Nonetheless, this scheme cannot perform better than the greedy selection on reducing the average network delay and the path oscillation in the multipath routing.

Besides, the ARAS model has some further applications about improving the WSN network performance. Ref. [15] proposed a layered routing scheme based on the model in the WSN by clustering. In the scheme, a data gathering layer [16] is made up of the sensor nodes in each cluster, and a routing layer is composed of all the cluster heads in the WSN. Then, dynamical selection for each cluster head in the data gathering layer and next hop in the routing layer can be optimized through the ARAS model. In the same way, Ref. [17] also proposed a layered future mobile network management mechanism is proposed based on the ARAS model by clustering. Also, the ARAS model can also improve the network performance through adaptively controlling the topology of the mobile networks in [18], for example, the energy efficiency and the transmission robustness. Nevertheless, although these studies [15,17,18] propose the novel schemes with the ARAS model, they all do not compare the performance with the greedy scheme in the corresponding scenarios.

In terms of the path oscillation problem caused by the greedy path selection, the aforementioned studies [7,14,15,17,18] based on the ARAS model can not solve it. Therefore, we propose the path selection model (WARAS) to alleviate the side effect of this problem. Also, these related works do not propose how noise stochastically affects the selection. By supposing the uniform stochastic effect of the noise on each path between each couple of the source and destination nodes, we derive a novel attractor expression containing the noise, which can characterize the noise's stochastic effect on the path selection.

3 Basic ARAS model and its drawbacks

In the changing nutrition environments, the *E. coli* cell can adaptively regulate its metabolism behaviors, and this process can be modeled [8] by the bi-attractor equations with noise items as follows:

$$\begin{cases} \dfrac{\mathrm{d}m_1}{\mathrm{d}t} = \dfrac{S(A)}{1+{m_2}^2} - D(A)m_1 + \eta_1, \\ \dfrac{\mathrm{d}m_2}{\mathrm{d}t} = \dfrac{S(A)}{1+{m_1}^2} - D(A)m_2 + \eta_2, \end{cases} \tag{1}$$

where m_1, m_2, respectively, denote the concentrations of the cell's two different kinds of mRNA, which can also equivalently denote the concentrations of two different kinds of the protein because of the transcription mechanism between mRNA and protein. Eq. (1) presents the formula about the mRNA concentration rates. η_i denotes the noise, which specifies all kinds of the internal and external factors that affect the cell's metabolism. A denotes the cell's *activity*, which specifies the cell's adaptation goodness to the environments. Then, $S(A)$ and $D(A)$ denote, respectively, the protein's synthesis rate and the decomposition rate, which are both proportional to the *activity* A. It is well known that an active cell can metabolize more vigorously than the inactive one, and also its immunity is stronger. Similarly in

the equations, when the cell becomes active, the mRNA concentration rates become high because of the increasing $S(A)$ and $D(A)$. At the same time, the increasing $S(A)$ and $D(A)$ make the non-noise items of (1) increase, so the effect of the noise on the concentration rate is reduced relatively. Also, the active cell probably conducts the cell division, so the synthesis rate is supposed to be faster than the decomposition rate.

We can deduce the attractors of (1) without the noise items according to the condition $\frac{\mathrm{d}m_i}{\mathrm{d}t} = 0,\ i = 1, 2$. A theorem about the attractors, Theorem 1, can be obtained based on the condition.

Theorem 1. If $m \neq 0$, $D(A) \neq 0$, and $\frac{S(A)}{D(A)} > 2$, two attractors can be derived from (1) without the noise items, that is, $(m, \frac{1}{m})$ and $(\frac{1}{m}, m)$. Otherwise, the equations have only one attractor, that is, (m, m).

Proof. To get the attractors of (1) without the noise items, Eq. (2) can be obtained as follows through the equations $\frac{\mathrm{d}m_i}{\mathrm{d}t} = 0,\ i = 1, 2$:

$$\begin{cases} m_1(1 + {m_2}^2) - \dfrac{S(A)}{D(A)} = 0, \\ m_2(1 + {m_1}^2) - \dfrac{S(A)}{D(A)} = 0. \end{cases} \tag{2}$$

Then, we can get $m_1(1 + {m_2}^2) = m_2(1 + {m_1}^2)$ from (2), so the relationship of m_1 and m_2 in (2) is $m_1 = \frac{1}{m_2}$ or $m_1 = m_2$.

If $m_1 = \frac{1}{m_2}$, we can reduce (2) and obtain a sufficient condition $\frac{S(A)}{D(A)} \geqslant 2$ that Eq. (1) without the noise items has one real attractor. When $\frac{S(A)}{D(A)} = 2$, we can obtain $m_1 = m_2 = 1$ from (2). Thus, Eq. (1) without the noise items has an attractor as $(1, 1)$. When $\frac{S(A)}{D(A)} > 2$, $m_1 + \frac{1}{m_1} > 2$ and $m_2 + \frac{1}{m_2} > 2$ from (2) can be obtained. So apparently, Eq. (1) without the noise items has two different attractors that satisfy $m_1 = \frac{1}{m_2}$.

If $m_1 = m_2$, we can get the cubic equations ${m_1}^3 + m_1 - \frac{S(A)}{D(A)} = 0$ and ${m_2}^3 + m_2 - \frac{S(A)}{D(A)} = 0$. Then, by the discriminant $\Delta = (\frac{S(A)}{2D(A)})^2 + \frac{1}{27} > 0$, Eq. (2) has a real root that satisfies $m_1 = m_2$. Hence, Eq. (1) without the noise items has only one attractor (m_1, m_2) that satisfies $m_1 = m_2$. Thus, Theorem 1 holds.

Eq. (1) models the adaptation behaviors of the *E. coli* cell to the dynamic nutrition environments. If the nutrition condition changes, the cell shifts its state according to its current *activity*. When the *activity* is so high that the noise items cannot affect the mRNA concentration rates, the cell still stays in the current state. On the contrary, when the current *activity* gets so low that the effect of the noise on the metabolism rate cannot be neglected, the cell's state will shift stochastically. Because the mRNA concentrations become stochastic under the effect of the noise, the *E. coli* has the opportunity to regain the adaptation to the new environment. Subsequently, if one state makes the cell's *activity* rise so greatly that the metabolism can ignore the noise's effect, the state of the cell becomes stable and adapts to the new environment.

The *E. coli* and the sensor node have many similar characteristics. For example, both of them are independently distributed in the complex environments and have to adapt to the environments by regulating their states themselves. However, when the ARAS model applies into the path selection of the WSN multipath routing, there still exist three drawbacks. The first one is how to define the *activity* to reflect the adaptation goodness of the multipath transmission to the dynamic network environments, the second one is that how each sensor node adaptively selects its working path toward the corresponding destination, and the last one is how the noise affects the path selection stochastically. In the next section, we introduce the proposed solutions for the three drawbacks. The solution for the first drawback is proposed in the subsection of the novel expression of the *path-activity*, the second one in the subsection of the definition of selection probability for each path selected as the working path, and the last one in the subsection of the variation relationships among the noise, selection probability, and *path-activity*. Besides, it is noted that only one path is used for the data transmission every moment between each couple of the sensor and sink nodes in the proposed model. For convenience, this path is called the working path in the following description.

4 WARAS: an adaptive path selection model for WSN inspired by ARAS

4.1 The multi-attractor equations for WARAS

To model the adaptation of the multipath traffic transmission to the dynamic network environments, the multi-attractor equations in [7] are adopted. With the equations, we propose an adaptive path selection model for WSN multipath transmission, namely *WARAS*. The equations are shown as follows:

$$\begin{cases} \dfrac{\mathrm{d}m_1}{\mathrm{d}t} = \dfrac{S(A)}{1+\hat{m}-{m_1}^2} - D(A)m_1 + \eta_1, \\ \dfrac{\mathrm{d}m_2}{\mathrm{d}t} = \dfrac{S(A)}{1+\hat{m}-{m_2}^2} - D(A)m_2 + \eta_2, \\ \quad\vdots \\ \dfrac{\mathrm{d}m_n}{\mathrm{d}t} = \dfrac{S(A)}{1+\hat{m}-{m_n}^2} - D(A)m_n + \eta_n, \end{cases} \tag{3}$$

where the m_i denotes the transmission quality of the ith path between each couple of the source node and destination nodes in WSN. The $\hat{m}$ denotes the best transmission quality among the multipaths, that is, $\hat{m} = \max_i\{m_i,\ i = 1, 2, \ldots, n\}$. The A denotes the *path-activity*, which specifies the adaptation goodness of the traffic transmission between each source and destination pair to the real-time network environments. The $S(A)$ and $D(A)$ are, respectively, the path quality promoter and inhibitor, both of which are proportional to the *path-activity*. Because the increasing *path-activity* can improve the path transmission quality, the promoting rate of $S(A)$ must exceed the inhibiting rate of $D(A)$. η_i denotes the noise, which can cause some local random fluctuations of m_i. Here, the effect of the noise is supposed to be transient and within a small range of m_i. In fact, the noise represents an integration of the factors taking the stochastic effect on the path transmission quality, for example, the short-time WSN traffic and the random failures of WSN equipment.

Subsequently, by supposing the noise affecting each m_i identical, that is, $\eta = \eta_i$, $i = 1, 2, \ldots, n$, we deduce a new attractor expression with the noise. According to the equations $\frac{\mathrm{d}m_i}{\mathrm{d}t} = 0$, $i = 1, 2, \ldots, n$, the novel attractors $(m_1, m_2, \ldots, m_i, \ldots, m_n)$ can be obtained, whose components are expressed as follows:

$$m_i = \begin{cases} \dfrac{1}{2}\left(\sqrt{\left(\dfrac{S(A)+2\eta}{D(A)}\right)^2 + 4} - \dfrac{S(A)}{D(A)}\right), & i \neq k, \\ \dfrac{S(A)+\eta}{D(A)}, & i = k. \end{cases} \tag{4}$$

Here, the attractor is composed of a special component $m_k = \frac{S(A)+\eta}{D(A)}$ and the other same components $m_{i\neq k}$, where k denotes the index of the special component. Subsequently, we prove the following theorem about the number of the attractors in (3) under the condition of $\eta = \eta_i$.

Theorem 2. If $S(A) \neq 0$, $D(A) \neq 0$, and $\eta = \eta_i$, $i = 1, 2, \ldots, n$, the necessary and sufficient condition that (3) has more than one attractor is $\frac{D(A)^2 - 2S(A)^2}{2S(A)} \neq \eta$.

Proof. If (3) has only one attractor in the case of $\eta = \eta_i$, the attractor must be $(m, m, \ldots, m)$, where $m = m_i$, $i = 1, 2, \ldots, n$. Therefore, with (4), we can acquire $m_{i\neq k} = m_k$. Then, we reduce it to get $\eta = \frac{D(A)^2 - 2S(A)^2}{2S(A)}$. Thus, Theorem 2 holds.

In WARAS, each attractor can be considered to be a stable adaptation state of the multipath transmission. Then, it is expected the adaptation state can be always achieved no matter how the network environment changes. Here, the adaptation state is expressed due to the performance demands, for example, load balancing, congestion avoidance, robustness, and reliability. In detail, when the *path-activity* declines, the effect of the noise on the adaptation state rises. Then, the multipath transmission regains a stable adaptation state through the stochastic effect of the noise on the original state. On the contrary, the effect of the noise decreases with the increasing *path-activity*. Because of escaping from the stochastic

effect of the noise, the stable adaptation state of the multipath transmission can be kept. According to (4), we can perform the adaptation process and conclude a corollary as follows.

Corollary 1. If the *path-activity* increases, m_k rises and $m_{i\neq k}$ declines. Meanwhile, the effect of the noise is negligible. Otherwise, m_k declines and approaches $m_{i\neq k}$. Furthermore, the stochastic effect of the noise on the transmission state becomes strong and cannot be ignored with the decreasing *path-activity*.

Proof. In (3), both the promoter $S(A)$ and the inhibitor $D(A)$ are proportional to the *path-activity*, and the promoting rate of $S(A)$ exceeds the inhibiting rate of $D(A)$. Hence, the effect of the noise in (4) is negligible with the sufficient increasing *path-activity*. Also, because the noise only leads to some small local fluctuations, m_k rises in the meanwhile. Then, if we might as well ignore the noise items in (4) and let $\omega = \frac{S(A)}{D(A)}$, then $m_{i\neq k} = \frac{4}{\sqrt{\omega^2+4}+\omega}$. Because ω goes up with the increasing *path-activity*, $m_{i\neq k}$ declines. On the contrary, if the *path-activity* decreases, $S(A)$ and $D(A)$ both decline. Thus, apparently in (4), the effect of the noise on the attractor becomes strong and cannot be ignored with the sufficient decreasing $S(A)$ and $D(A)$. Because the rate of $S(A)$ exceeds the rate of $D(A)$, m_k declines correspondingly. Then, the decreasing *path-activity* makes $S(A)$ approach $D(A)$, so η approaches $\frac{D(A)^2-2S(A)^2}{2S(A)}$. Therefore, according to Theorem 2, m_k approaches $m_{i\neq k}$.

Subsequently, in the WSN multipath routing, the adaptation transmission state can be achieved through the adaptive path selection model in (3). However, we first need to determine the expression of the *path-activity*.

4.2 The novel expression of *path-activity*

In our proposed model, the *path-activity* is a metric that features the adaptation goodness of the data transmission between each couple of the source and destination nodes to the real-time network environments. To reflect the real-time adaptive state of the data transmission as far as possible, we improve the *activity* expression with the fixed points in [7] and define a continuous expression form for the *path-activity* as follows:

$$A = f(|Q_{\text{working}} - \hat{m}|). \tag{5}$$

Here, Q_{working} denotes the transmission quality of the working path of the source node toward the destination, and $\hat{m}$ is the best transmission quality, for example, the minimum path delay, the shortest path length, and the best reliability. $f(\cdot)$ is a function which is inversely proportional to $|Q_{\text{working}} - \hat{m}|$. That is to say, if the working path quality gets closer to the best path quality, the *path-activity* becomes higher. Otherwise, the *path-activity* becomes lower. Subsequently, we define a concrete expression for the *path-activity* in (6), and through this formula, we perform the dynamic-adaptive characteristic analysis and the network simulation for the proposed model in the following sections:

$$A = \frac{\gamma}{\alpha|Q_{\text{working}} - \hat{m}|^{\theta} + \beta}, \tag{6}$$

in this formula, α, β, γ, and θ are all positive constants.

In (6), when the quality of the working path achieves the maximum, that is, $|Q_{\text{working}} = \hat{m}|$, the *path-activity* also reaches its maximum $A = \frac{\gamma}{\beta}$. More obviously, the *path-activity* variations are presented in Figure 1, where the bound of the *path-activity* is set in the range from 0 to 10 by $\beta = 1$, $\gamma = 10$, and Partial Difference $= |Q_{\text{working}} - \hat{m}|$. Figure 1 shows the effect of θ on the *path-activity* by fixing the value of α, and the effect of α on the *path-activity* by fixing the value of θ. Basically, we can modify these constants to obtain the suitable formula of the *path-activity* for the model in a simulation. Generally in various network scenarios or services, quality of service (QoS) demands are very different. The transmission adaptation states also differ in thousands of ways. So, we need to modify the *path-activity* to fit the adaptation state, where β and γ are used to specify the bound of the *path-activity*. Besides, we can prolong the transmission time of the working path by increasing the range of the high *path-activity* with α and θ. The transmission quality of the working path fluctuates under the effect of the noise in the WSN network environments. Furthermore, the higher the *path-activity* is, the bigger the possibility is that the working path is kept. Therefore, the bigger range of the high *path-activity* can neglect more fluctuations

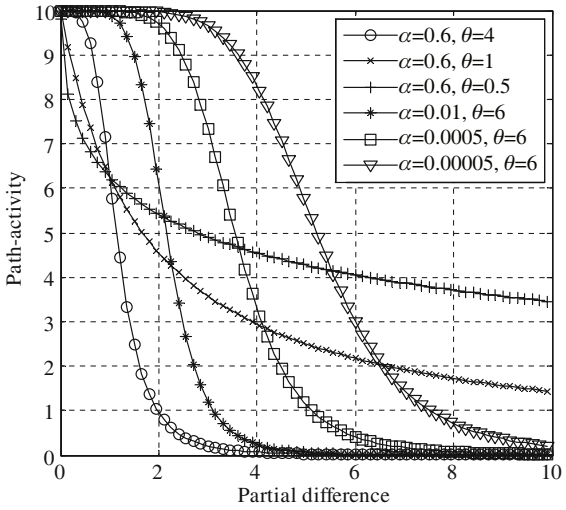

Figure 1 The variations of *path-activity* under different constraint parameters.

of the path quality and makes the working path transmit for a longer time. As shown in Figure 1, the range of the high *path-activity* can be extended by reducing the value of α.

4.3 The definition of selection probability for each path selected as the working path

In the multipath routing, the traffic transmission between each couple of the source and destination nodes can be regulated by shifting their working path among several candidate paths according to the transmission quality of these paths. In our proposed model, the *path-activity* is used to reflect the multipath transmission quality for regulating the transmission. When the *path-activity* is sufficiently high, the traffic transmission will continue. On the contrary, the transmission needs to be improved by reselecting the working path. Because of the burstiness and intermittency characteristics of the WSN network traffic, randomization [14,19] is considered as an effective strategy to optimize the load balancing and the congestion control for the multipath selection. The greedy path selection always easily makes the best quality path a network hotspot and causes the congestion in the hotspot. Thus, the randomization of the path selection can effectively reduce the possibility that the hotspot is formed, which is helpful to avoid the network congestion and balance the network load. Then, in our model, the stochastic path selection is also used to improve the transmission efficiency. Concretely, each path is selected as the working path in this paper by a selection probability continuously proportional to the corresponding path transmission quality. Specially, the selection probability is defined as $P_i = \frac{m_i}{\sum_{j=1}^{n} m_j}$ according to (4). Especially, each source and destination pair is expected to transmit their traffic through the best quality path, so the selection probability that the working path is kept is set as $P_k = \frac{m_k}{\sum_{j=1}^{n} m_j}$. Here, it is the probability that the path is selected as their working path again.

4.4 The variation relationships among noise, selection probability and *path-activity*

Subsequently, we investigate the variation relationships among noise, selection probability, and *path-activity* in a case that a source node gets five paths for the transmission. Figure 2 shows the variation relationships among them under the case, where $P_{\text{working}} = P_k$ denotes the selection probability that the working path is kept by the source node and $P_{\text{candidate}}$ denotes the selection probability that the other candidate paths (non-working paths) are selected as the working path. In (3), the path quality promoter and inhibitor are both proportional to the *path-activity*, and the promoting rate is higher than the inhibiting rate. Furthermore, the noise affects the path quality in random within a small range. Therefore, for the convenience of the following analysis, we set an instance of the multi-attractor equations based on the characteristics of the promoter, the inhibiter, and the noise, as shown in (7). The selection

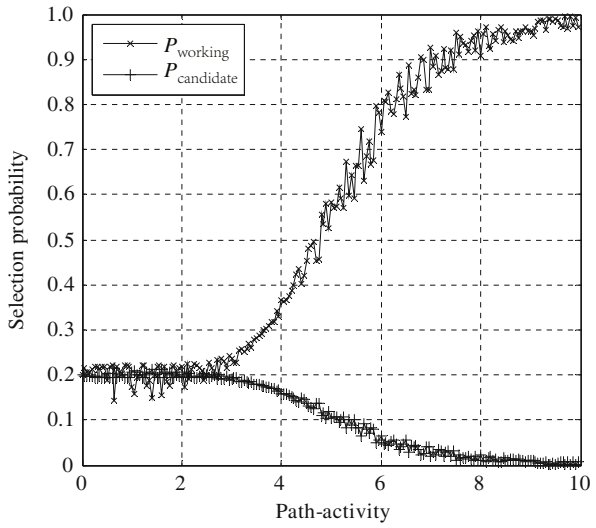

Figure 2 The variation relationships among noise, selection probability, and *path-activity*.

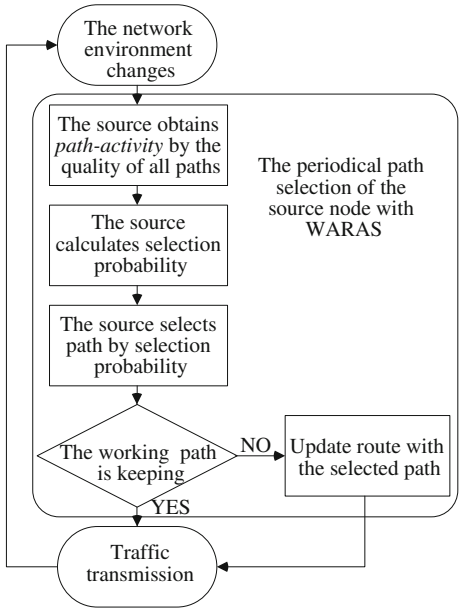

Figure 3 The implementation of the adaptive path selection operation in a source node.

probabilities in Figure 2 are calculated with the instance.

$$\begin{cases} \dfrac{\mathrm{d}m_1}{\mathrm{d}t} = \dfrac{A(0.006A^4+1)}{1+\hat{m}-{m_1}^2} - 2A\cdot m_1 + \mathrm{rand}(0,1), \\ \dfrac{\mathrm{d}m_2}{\mathrm{d}t} = \dfrac{A(0.006A^4+1)}{1+\hat{m}-{m_2}^2} - 2A\cdot m_2 + \mathrm{rand}(0,1), \\ \quad\vdots \\ \dfrac{\mathrm{d}m_n}{\mathrm{d}t} = \dfrac{A(0.006A^4+1))}{1+\hat{m}-{m_n}^2} - 2A\cdot m_n + \mathrm{rand}(0,1), \end{cases} \tag{7}$$

where $\mathrm{rand}(0,1)$ is a function to generate an arbitrary random number between 0 and 1.

Figure 2 shows the effect of the selection probability and the noise on the path selection. When the transmission quality of the working path between a couple of source and destination nodes becomes better, the *path-activity* in (5) increases. In the meanwhile, the component m_k of the attractor increases according to Corollary 1. Then, the selection probability P_{working} goes up, as shown in Figure 2. Thus, due to the increasing selection probability, the possibility rises that the working path is kept, and the effect of the noise on the path selection can be gradually neglected. On the contrary, when the transmission quality of the working path becomes worse, the *path-activity* decreases correspondingly. Then, because all the components of the attractor in (4) become average according to Corollary 1, the selection probabilities of all candidate paths also tend to become uniform. In Figure 2, when the *path-activity* declines sufficiently, the P_{working} approaches the $P_{\text{candidate}}$. Furthermore, the noise determines the variations of all the selection probabilities. As a result, the working path will be reselected mostly depending on the effect of the noise. Finally, the stochastic characteristic can help each source and destination pair to rediscover the adaptive working path. Here, it is noted that the merits of the path quality mentioned are relative to the best transmission quality in (5).

Based on the relationship analysis, we can present the path selection operation in the proposed model, which is shown in Figure 3. It can be seen from the figure the periodical path selection is performed in each source node, and each candidate path is selected as the working path by the corresponding selection probability. Then, if the working path is kept, the traffic transmission continues. Otherwise,

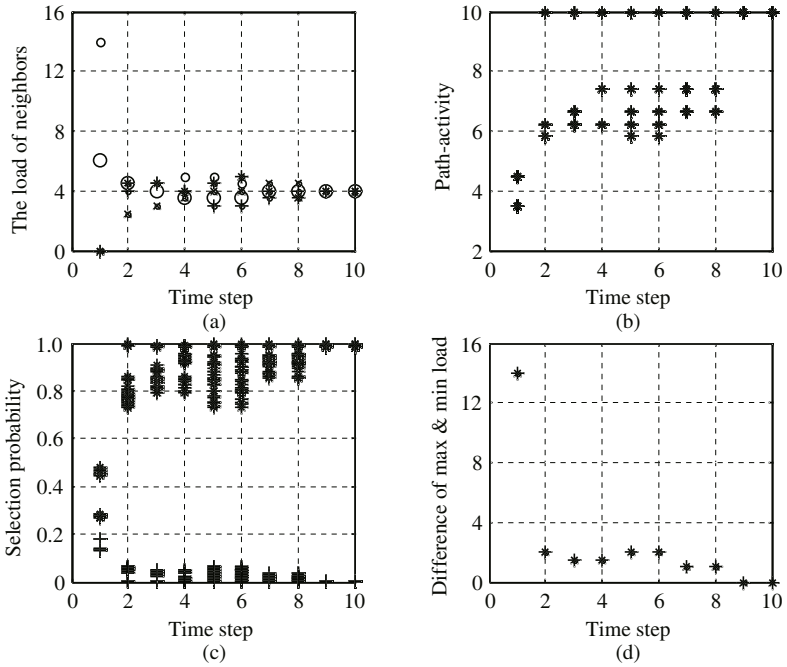

Figure 4 A dynamic-adaptive selection demonstration of WARAS under the illustrative WSN layout. (a) Load variation of neighbors; (b) *path-activity* variation; (c) selection probability variation; (d) load difference variation.

the route table will be updated with the selected path. In fact, the operation in Figure 3 is linear with low calculation complexity, which can be performed very fast.

4.5 The dynamic-adaptive selection characteristic analysis of WARAS

In this section, we investigate the dynamic and adaptive selection characteristic of WARAS. For this purpose, we take an illustrative WSN layout as an experimental scenario composed of many source nodes and their shared neighbor nodes, where each source node will select one next hop from these neighbor nodes for the traffic transmission. In the scenario, if a neighbor node is selected as a next hop by a source node, the load of the neighbor node will increase. Furthermore, each source node can only use a neighbor node as its next hop every moment, and at the same time, it can also acquire the load level of each neighbor node every moment. Besides, in the experiment, the time is divided into many time steps, and at each time step, each source node selects its next hop from the neighbor nodes according to the operation in Figure 3. In the operation, the *path-activity* in (6) is expressed here by the load of the neighbor nodes, where Q_{working} denotes the load of each source node's next hop, and $\hat{m}$ denotes the minimum load among the neighbor nodes. Subsequently, to highlight the dynamic-adaptive characteristic of our proposed model, we set a worse load distribution condition at the beginning of the experiment, where each source node selects its next hop from two neighbor nodes in uniform random. After that, each source can select the next hop from all the neighbor nodes. In the meantime, the load level of each neighbor node is quantized for convenience, and set as 0 in the beginning of the experiment. Also, it is supposed, if a neighbor node is selected as a next hop by a source node, the load of the neighbor is increased by 0.5. When a neighbor node is selected by all the source nodes as their next hops, it reaches its maximum load.

Subsequently, we first make a demonstration of the effect of the WARAS model on the load of the neighbors in a concrete scenario composed of 40 source nodes and 5 neighbor nodes. Figure 4 shows the load variation process of the neighbor nodes in 10 time steps, which is modeled by (7). To observe the adaptive selection process, we show some parameter variations of our proposed model in Figure 4, for example, the *path-activity*, the selection probability, and the difference between the max and min load levels among all neighbor nodes. From Figure 4(a), it can be seen that all the neighbor nodes reach the

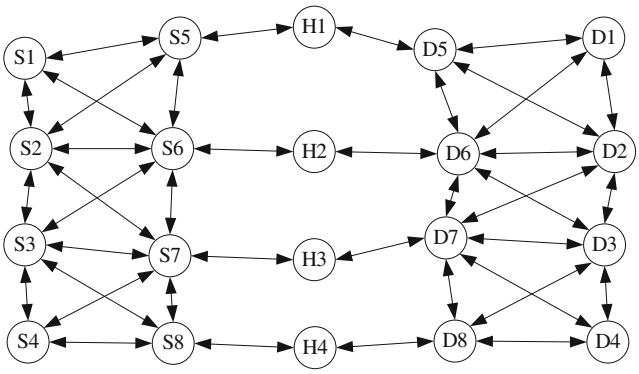

Figure 5 The layout of the network simulation scenario.

identical load at last. In the meantime, the *path-activity* of all source nodes attains the maximum in Figure 4(b), where the *path-activity* is bounded within the range from 0 to 10. It is consistent with the load result in Figure 4(a). Figure 4(c) shows the overall variations of the selection probabilities in all the source nodes, where they gradually tend to stabilization with the increasing time steps. Concretely, the selection probability goes to 1 that the next hop of each source node is kept, which is marked by the asterisk in Figure 4(c). The selection probability goes to 0 that each other neighbor node (non-next-hop node) is selected as one next hop, which is marked by plus in Figure 4(c). Also, Figure 4(d) shows the variations of the difference between the max and min load of all neighbor nodes. It can be seen from the figure that the difference approaches 0 with the increasing time steps. Thus, it is also consistent with the load variations in Figure 4(a). As a result, it is evident the WARAS can regulate the load distribution of all the neighbor nodes dynamic-adaptively under the WSN layout. Besides, if a neighbor node can represent a path, our proposed model can select the working path dynamic-adaptively in the WSN multipath routing. Furthermore, it is expected our model can behave better on reducing the network delay and the path oscillation than the greedy scheme. Therefore, in the section, we validate the expectation in a platform (called optimizing the performance of the network (OPNET)).

5 Simulations

5.1 Simulation scenario setup

To investigate the efficiency of WARAS in the complex network conditions, we use a network simulation platform OPNET. In the platform, a multipath routing protocol is implemented by modifying the single path routing AODV. We simulate the multipath routing in a scenario that 46 nodes are homogeneously distributed in a 2 km $\times$ 2 km area within some sensor nodes and sink nodes. Its basic layout is shown in Figure 5, where S_i $(i = 1, 2, 3, \dots)$ denote the sensor nodes which have some data to be delivered and forwarded, and D_i $(i = 1, 2, 3, \dots)$ denote the sink nodes. To facilitate the probe of the path quality, we set four hotspot nodes H_i $(i = 1, 2, 3, 4)$ to make all of routing paths pass through them. Due to the burstiness and intermittency of the WSN network traffic, each sensor node is set to send the data packets with an exponential distribution time in the simulation, and the size of the packets is also set with an exponential distribution in the packet generation. Specifically, the traffic of each source node in Figure 5 is generated with the distribution Exponential (1), where Exponential (1) denotes the exponential distribution with the mean packet inter-arrival time of 1 s. Furthermore, every 5 min, the sources in the layout are set to send the data packets with the packet inter-arrival time distribution Exponential (0.1) for 15 min. Consequently, the simulation will be executed in an hour, so each source sends the data packets with the inter-arrival time distribution Exponential (0.1) 3 times.

Besides, to validate the adaptation of WARAS to the dynamic network environments, the simulation is performed in five different scenarios. In these scenarios, the four hotspots are, respectively, set the different processing capabilities. In OPNET, the processing capacity of a network node is specified by a

Table 1 Scenario parameters

Parameter	Value	Parameter	Value
The number of nodes	46	Allowed hello loss	10
The size of area (m^2)	2000×2000	Datagram forwarding rate (DFR)	40,50,60,70,80,90,100,110
Transmission radius (m)	500	Packet inter-arrival time (s)	Exponential (1), Exponential (0.1)
Destination only flag	Enabled	Simulation time (min)	60

parameter datagram forwarding rate (DFR, packets/s), which indicates the maximum number of packets forwarded by the node per unit time. The processing capacities of the four hotspots H_i $(i = 1, 2, 3, 4)$ are set, respectively, in the five scenarios, which are Sc1(DFR : $70, 70, 70, 70$), Sc2(DFR : $70, 60, 50, 40$), Sc3(DFR : $90, 80, 70, 60$), Sc4(DFR : $110, 100, 90, 80$), and Sc5(DFR : $110, 100, 50, 40$). Here, Sci $(i = 1, 2, \ldots, 5)$, respectively, indicate the five different scenarios. At the same time, DFRs of all the source and destination nodes are set as 70 packets per second in these scenarios. We will simulate the multipath routing with the adaptive path selection model WARAS in the five simulation scenarios. Also, for comparison, the greedy path selection will also be used in the multipath routing in the meanwhile. The parameters of these scenarios are summarily listed in Table 1, where the extra nodes not shown in Figure 5 are the source and destination nodes.

5.2 The path quality probe

In the multipath routing, the path selection should be performed periodically to make the data transmission between each couple of the source and destination nodes adapt to the real-time network environments. Furthermore, each source needs to acquire the real-time transmission quality of each path toward its destination for the path selection. So, the packet feedback mechanism is adopted, where each destination node sends a feedback packet to the corresponding source node for each arrival data packet to inform of the path quality, for example, the path delay. Based on the mechanism, the path quality probe of all the paths between each couple of the source and destination nodes can be performed before each path selection.

In AODV, each path has a lifetime. If one path does not receive the routing update message or forward any traffic in its lifetime, the path will be set invalid. As a result, if the path quality probe always extends the lifetime of the paths, the frequent route rediscoveries make the multipath routing suffer the worse performance even than the single path routing. Therefore, the path quality probe of all the paths should be completed in the lifetime of these paths. In the AODV, there are two measures that affect the lifetime of each path, the route entry timeout, and the HELLO timeout. To keep the path alive as long as possible, we ignore the route failure caused by the route entry timeout. Thus, the HELLO timeout is the main factor that affects the lifetime of each path. Because the data transmission in each path can prolong a period for the path lifetime in the routing protocol, we can perform the path quality probe in this period to avoid path failure caused by the probe feedback waiting. In the multipath routing, this period is set as the period of *Allowed Hello Loss*, which is the time threshold in OPNET that causes the HELLO timeout. Furthermore, we will also perform the path selection in the interval of the *Allowed Hello Loss*. Besides, to guarantee the successful quality probe of each path, each probe feedback packet is set a feedback waiting threshold. Once a path probe packet is sent to a candidate path, a time threshold will be set for its feedback packet. If the feedback packet is received in the threshold, the quality probe of this path is finished. Otherwise, another probe packet will be sent to this path, but the feedback waiting threshold will be double. The path quality probe will continue until all candidate paths are probed or the *Allowed Hello Loss* time expires. In general, the initial feedback time threshold can be set as twice the candidate path delay. However, if the path does not record the path delay information in the beginning of simulation, it can be set a value roughly before the period of *Allowed Hello Loss*. Based on this method, each source can perform the path quality probe of all candidate paths to its corresponding destination.

When the path quality probe is performed, the source node reselects its working path according to the quality of all the paths toward its destination. Subsequently, if the source finishes the path selection,

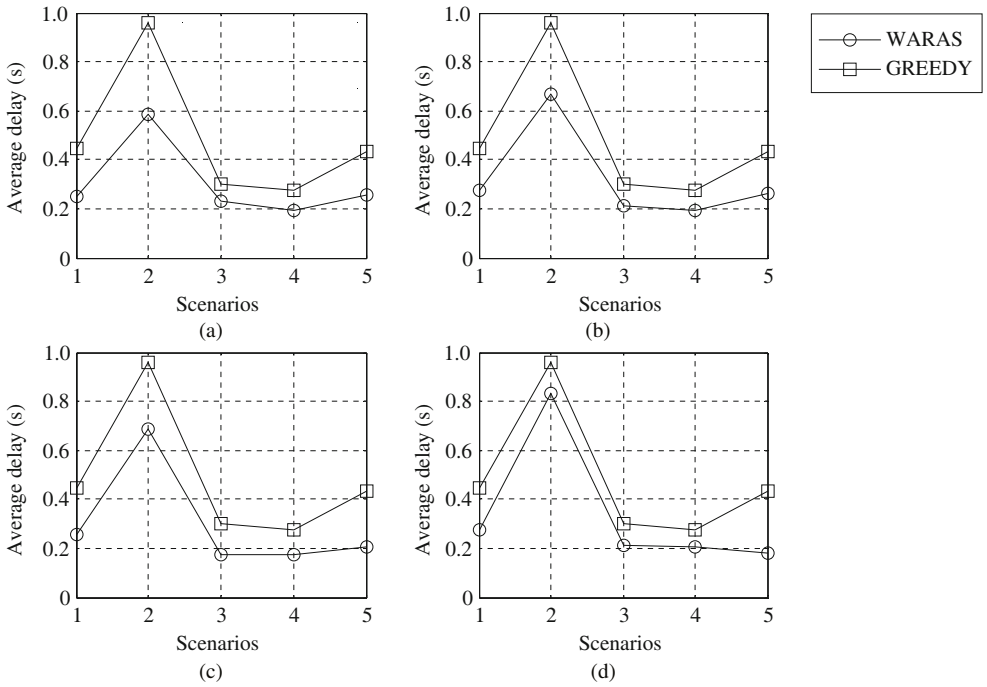

Figure 6 The average WSN network delay comparison of the two path selection schemes in the five simulation scenarios by probing the path delay. (a) $\alpha = 1.2 \times 10^{-4}$; (b) $\alpha = 6 \times 10^{-4}$; (c) $\alpha = 0.008$; (d) $\alpha = 0.04$.

the next path selection period will restart. In the multipath routing, the path quality probe, the path selection, the route discovery, and the data transmission are all performed in each source node. Besides, we do not basically create additional packets for the path quality probe. A path quality probe packet can be a data packet to be sent. With the aid of a flag that is set in the data packets, the destination can identify it and send a corresponding feedback packet. Then, the feedback packet can be a data packet to be sent or a high layer transmission control protocol (TCP) acknowledge (ACK) packet. However, if there is no ACK packet or data packet to be sent timely, a feedback packet only including path quality and destination-related information can be created for the source. Actually, the path quality probe is just periodically carried out under the demand of traffic transmission, which increases the WSN throughput less. In the following simulation, the path transmission quality will be expressed, respectively, by the path delay and the max node packet arrival rate of each path, which are obtained with the path quality feedback packets. Then, the parameter configuration of WARAS is the same with the numerical experiments in the last section except θ and α in the *path-activity* formula (6). Because we also investigate the effect of the different ranges of high *path-activity* on the networking performance, we might as well set a fixed θ as 6 to facilitate the range adjustment.

5.3 Path selection by probing the path delay

Here, we use the path delay to measure the path transmission quality, where the path delay indicates the time elapsed between a data packet creation at its source and destruction at its destination. Apparently, the best path quality is the minimum path delay. Because WARAS evaluates the adaptation goodness of the multipath transmission between each couple of the source and destination nodes to the network environments by the *path-activity*, we investigate the effect of the different ranges of high *path-activity* on average network delay and working path oscillation rate in the five different network scenarios, respectively, in Figures 6 and 7. Here, we modify the range of the high *path-activity* with one of its parameters α in (6). Besides, the average network delay indicates the average of the WSN network delay in different simulation moments, and the oscillation rate means the shifting frequency of the working path among all the paths between each couple of the source and destination nodes.

Figure 6 compares the two path selection schemes on reducing the average network delay in the five

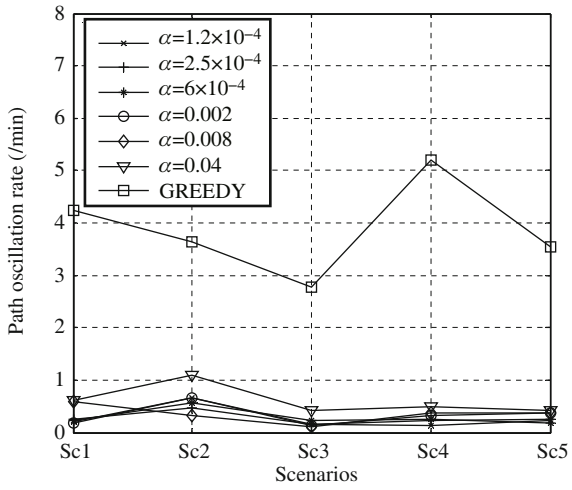

Figure 7 The working path oscillation rate comparison of the two path selection schemes in the five simulation scenarios by probing the path delay.

different network scenarios (Sc1, Sc2, Sc3, Sc4, Sc5), which are WARAS and the greedy path selection. The greedy path selection provides the path with the best transmission quality for each couple of the source and destination nodes as its working path for every path selection. It can be seen from the figure that the WARAS reduces the average network delay more than the greedy path selection. Besides, we also compare the oscillation rates of the working paths in the two path selection schemes in Figure 7 respectively, in the five different network scenarios. Because each self-organization source node in WSN selects its working path for each destination independently, the couple of the source and destination nodes in Figure 7 is picked randomly to reflect the oscillation situation of the working path in our scenarios. Evidently, it can be seen from Figure 7 that the WARAS can make the working path oscillation less frequent than the greedy path selection. Consequently, through selecting the working path with the WARAS according to the path delay, the average WSN network delay and the working path oscillation can be both reduced.

5.4 Path selection by probing the node packet arrival rates in each path

In this subsection, we use the packet arrival rate of the nodes in each path to measure the path transmission quality. Similarly, we compare the two path selection schemes in the five different network scenarios. Because the nodes in each path probably have different DFRs, real-time packet arrival situation in each node can be expressed by $\frac{\mathrm{PAR}}{\mathrm{DFR}}$. Here, the PAR denotes the packet arrival rate (packets/s) of each node in different simulation moments, which is periodically collected by each node in the simulation. Then, we use a formula $\frac{1}{\max_i\{\frac{\mathrm{PAR}_i}{\mathrm{DFR}_i}, i=1,2,\dots\}}$ to indicate the transmission quality of a path, where the PAR_i and DFR_i, respectively, denote the packet arrival rate and DFR of the ith node in the path. It is evident that best path quality is minimum $\max_i\{\frac{\mathrm{PAR}_i}{\mathrm{DFR}_i}, i = 1, 2, \dots\}$. Also, we also investigate the effect of the different ranges of high *path-activity* on the average network delay and the working path oscillation in the five different network scenarios, respectively, in Figures 8 and 9.

Figure 8 compares the two path selection schemes on reducing the average network delay in the five network scenarios according to the node packet arrival rates in each path, which are the WARAS and the greedy path selection. It can be seen from the figure that the WARAS can still reduce the average network delay more than the greedy selection. Figure 9 shows the WARAS reduces the working path oscillation more than the greedy selection between a couple of the source and destination nodes by probing the node packet arrival rates in each path. Therefore, the WARAS performs better similarly than the greedy selection on reducing the average network delay and the working path oscillation with the difference path quality metrics, the packet arrival rates. Furthermore, the results also show the reliability of our proposed model.

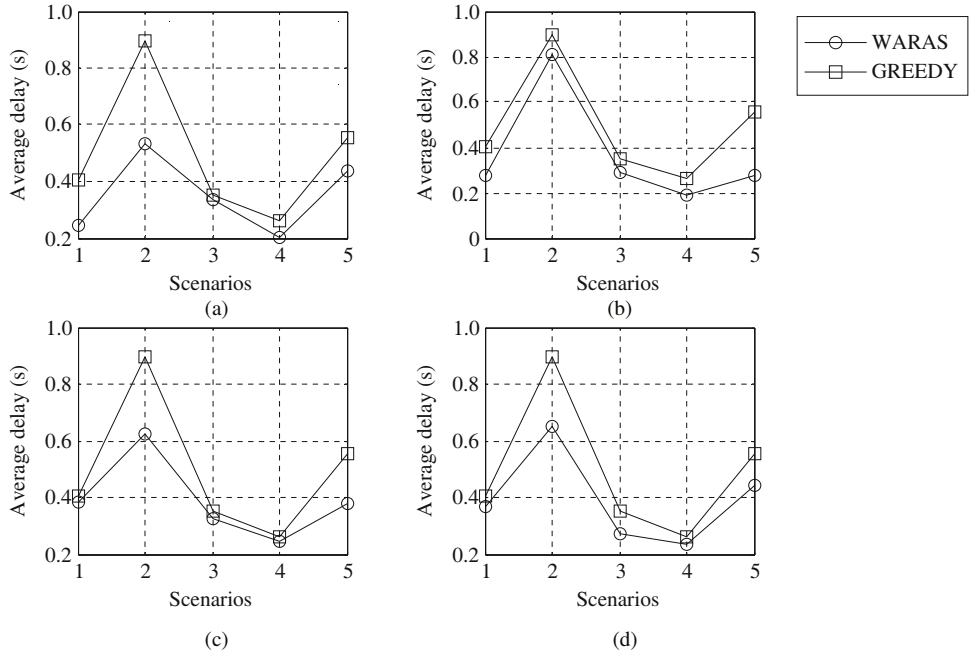

Figure 8 The average WSN network delay comparison of the two path selection schemes in the five simulation scenarios by probing the node packet arrival rates in each path. (a) $\alpha = 1.2 \times 10^{-4}$; (b) $\alpha = 6 \times 10^{-4}$; (c) $\alpha = 0.008$; (d) $\alpha = 0.04$.

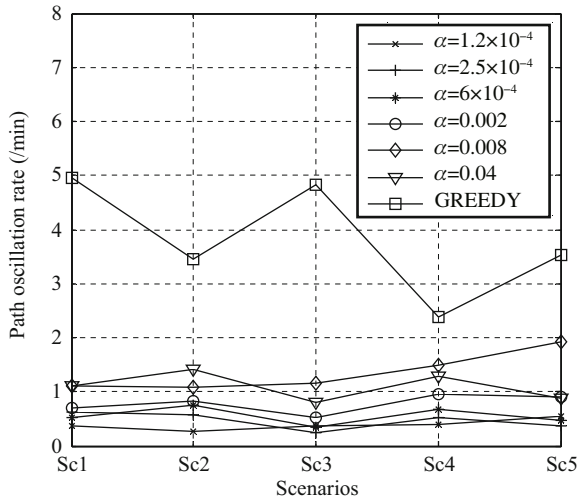

Figure 9 The working path oscillation rate comparison of the two path selection schemes in the five simulation scenarios by probing the node packet arrival rates in each path.

6 Conclusion

Inspired by the adaptation of the *E. coli* to the changing nutrition environments, a novel path selection model WARAS is proposed to improve the performance of WSN multipath transmission. In a multipath AODV protocol, our proposed model is verified to perform better about reducing the WSN network delay and the path oscillation than the greedy path selection with two path metrics, that is, the path delay and the max node packet arrival rate of each path. Besides, through more experiments, we found the multipath routing is not suitable to the networks with the frequent link failures caused by mobility, but the fixed networks, the few mobility networks, or the slow-moving networks. Specially, because the frequent path failures will not only undermine the path selection process, but also the repeated route discovery will cripple the network. Then, in the future work, we will discuss the effect of the other parameters in the WARAS in detail on the path oscillation, for example, the selection probability, the synthesis rate,

and the decomposition rate. Furthermore, we will also optimize the other network performance with the proposed model, for example, the QoS, the resource distribution, and management.

Acknowledgements

This work was supported by National Basic Research Program of China (973 Program) (Grant No. 2012CB315905), National Natural Science Foundation of China (Grant Nos. 60932005, 61172048, 61100184, 61201128), and National High-tech R&D Program of China (863 Program) (Grant No. 2013AA01A209).

References

1 Macit M, Gungor V C, Tuna G. Comparison of QoS-aware single-path vs. multi-path routing protocols for image transmission in wireless multimedia sensor networks. Ad Hoc Netw, 2014, 19: 132–141
2 Li W S, Tsai C W, Chen M, et al. Threshold behavior of multi-path random key pre-distribution for sparse wireless sensor networks. Math Comput Model, 2013, 57: 2776–2787
3 Liu A F, Zheng Z M, Zhang C, et al. Secure and energy-efficient disjoint multipath routing for WSNs. IEEE Trans Veh Technol, 2012, 61: 3255–3265
4 Liu A, Ren J, Li X, et al. Design principles and improvement of cost function based energy aware routing algorithms for wireless sensor networks. Comput Netw, 2012, 56: 1951–1967
5 Hong Y, Kim D, Li D, et al. Two new multipath routing algorithms for fault-tolerant communications in smart grid. Ad Hoc Netw, 2014, 22: 3–12
6 He S B, Li X, Chen J M, et al. EMD: energy-efficient delay-tolerant P2P message dissemination in wireless sensor and actor networks. IEEE J Sel Area Commun, 2013, 31: 75–84
7 Leibnitz K, Wakamiya N, Murata M. Biologically inspired adaptive multi-path routing in overlay networks. Commun ACM, 2006, 49: 62–67
8 Kashiwagi A, Urabe I, Kaneko K, et al. Adaptive response of a gene network to environmental changes by fitness-induced attractor selection. PLoS ONE, 2006, 1: e49
9 Borges V C M, Curado M, Monteiro E. Cross-layer routing metrics for mesh networks: current status and research directions. Comput Commun, 2011, 34: 681–703
10 Garroppo R G, Giordano S, Tavanti L. A joint experimental and simulation study of the IEEE 802.11s HWMP protocol and airtime link metric. J Commun Syst, 2012, 25: 92–110
11 Zhang J, Hu Z Y, Zhang T. Update chain-based approach for checking route oscillation of BGP. Chin J Aeronaut, 2011, 24: 202–209
12 Jose M C, Alberto G M, Marcelo B, et al. BGP-XM: BGP extended multipath for transit autonomous systems. Comput Netw, 2013, 57: 954–975
13 Guo L. LSSP: a novel local segment-shared protection for multi-domain optical mesh networks. Comput Commun, 2007, 30: 1794–1801
14 Leibnitz K, Wakamiya N, Murata M. Resilient multi-path routing based on a biological attractor selection scheme. In: Proceedings of the 2nd International Workshop on Biologically Inspired Approaches to Advanced Information Technology, Osaka, 2006
15 Sakhaee E, Leibnitz K, Wakamiya N, et al. Layered attractor selection for clustering and data gathering in wireless sensor networks. In: Proceedings of IEEE Wireless Communications and Networking Conference, Sydney, 2010. 1–6
16 He S B, Chen J M, Yau D K Y, et al. Cross-layer optimization of correlated data gathering in wireless sensor networks. IEEE Trans Mob Comput, 2012, 11: 1678–1691
17 Motoyoshi G, Leibnitz K, Murata M. Proposal and evaluation of a future mobile network management mechanism with attractor selection. J Wirel Commun Netw, 2012, 259: 1–13
18 Iwai T, Wakamiya N, Murata M. Error-tolerant and energy-efficient coverage control based on biological attractor selection model in wireless sensor networks. Int J Distrib Sens Netw, 2012, 2012: 971014
19 Dong M, Ota K, Li H, et al. RENDEZVOUS: towards fast event detecting in wireless sensor and actor networks. Computing, 2014, 96: 995–1010